Electronic Supplementary Material (ESI) for Lab on a Chip.

Supplementary Information†

Smartphone based Hand-Held Quantitative Phase Microscope using Transport of Intensity Equation Method

Xin Meng[1,‡], Huachuan Huang[2,3,‡], Keding Yan[4,‡], Xiaolin Tian[1], Wei Yu[1], Haoyang Cui[5], Yan Kong[1], Liang Xue[5,*], Cheng Liu[1,*], and Shouyu Wang[1,*]

[1]Department of Optoelectronic Information Science and Engineering, School of Science, Jiangnan University, Wuxi, Jiangsu 214122, China

[2]Institute of Fluid Physics, China Academy of Engineering Physics, Mianyang, Sichuan 621900, China

[3]School of Manufacturing Science and Engineering, Southwest University of Science and Technology, Mianyang, Sichuan 621010, China

[4]School of Electronic Information Engineering, Xi'an Technological University, Xi'an, Shaanxi 710032, China

[5]College of Electronics and Information Engineering, Shanghai University of Electric Power, Shanghai 200090, China

[‡]These authors contributed equally to this work.

[*]Corresponding authors: wsy_photonics@yahoo.com (S.W.); cheng.liu@hotmail.co.uk (C.L.); xueliangokay@gmail.com (L.X.)

Multi-Focal Imaging using Manual Focusing

With the smartphone used in our experiment, we could capture images focusing at different planes using the camera software. The focal plane can be adjusted by changing “Focus” value quantitatively and manually. In Figure S1(A), it shows multi-focal imaging capability of the smartphone. However, in order to avoid the field of view change and aberrations, in our experiment, we preferred small defocus interval between multi-focal intensities. Moreover, only information in central field of view (paraxial information) was adopted for phase retrieval. In our smartphone TIE experiments, Figure S1(B) shows the multi-focal imaging using manual focusing, which could focus on different imaging planes generating over-focus, in-focus and under-focus images. Thus according to TIE method, sample quantitative phase can be retrieved from these multi-focal images.

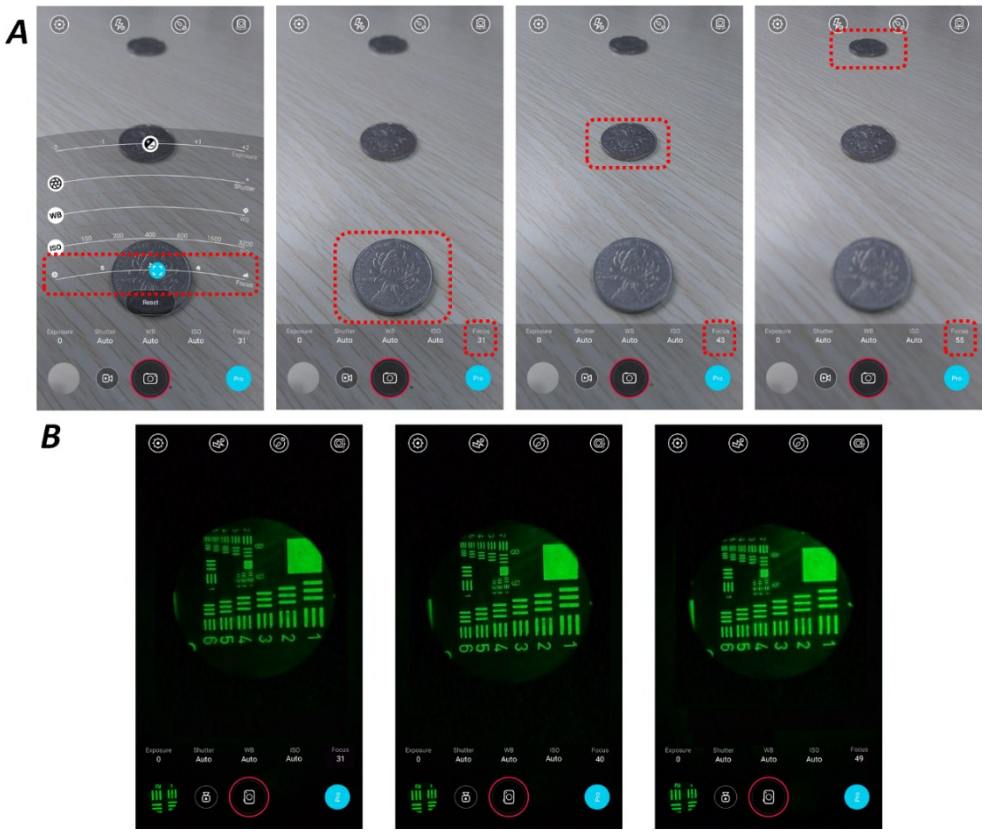

Figure S1. Multi-focal imaging using manual focusing. (A) Smartphone imaging. (B) Smartphone with micro-objective and eyepiece.

Defocus Distance Calibration

In phase retrieval via solving Poisson equation, defocus interval should be quantitatively calibrated in order to obtain high-accurate phase distribution. In this work, defocus calibration was done according to Figure S2. It is worth noting that in defocus calibration procedures, the smartphone based hand-held quantitative phase microscope system was separated as shown in Figure S2(A). However, positions of sample, micro-objective, eyepiece and smartphone were the same as the assembled quantitative phase microscope with 3-D printing shell. Firstly, the sample which is a 1951 USAF target (Edmund Optics, US) was set at the sample plane, after sample focusing, the in-focus image could be captured. Then, quantitative manual focusing was applied to shift the imaging plane, the captured intensity was changed into defocus image. Using the precision

translation stage (MT1-Z8, Thorlabs, US), the sample could be shifted along the optical axis. The accuracy of the precision translation stage can reach 0.1 μm. During the sample shifting along the optical axis, multiple intensities were recorded, representing images corresponding to various focal planes. Thus, according to focusing criteria [1,2], calculating Tamura coefficient of each captured intensity, the in-focus sample plane could be determined as well as the moving distance of the sample. The moved interval is the effective defocusing distance in the sample plane. The whole defocus distance calibration process is shown in Figure S2(B).

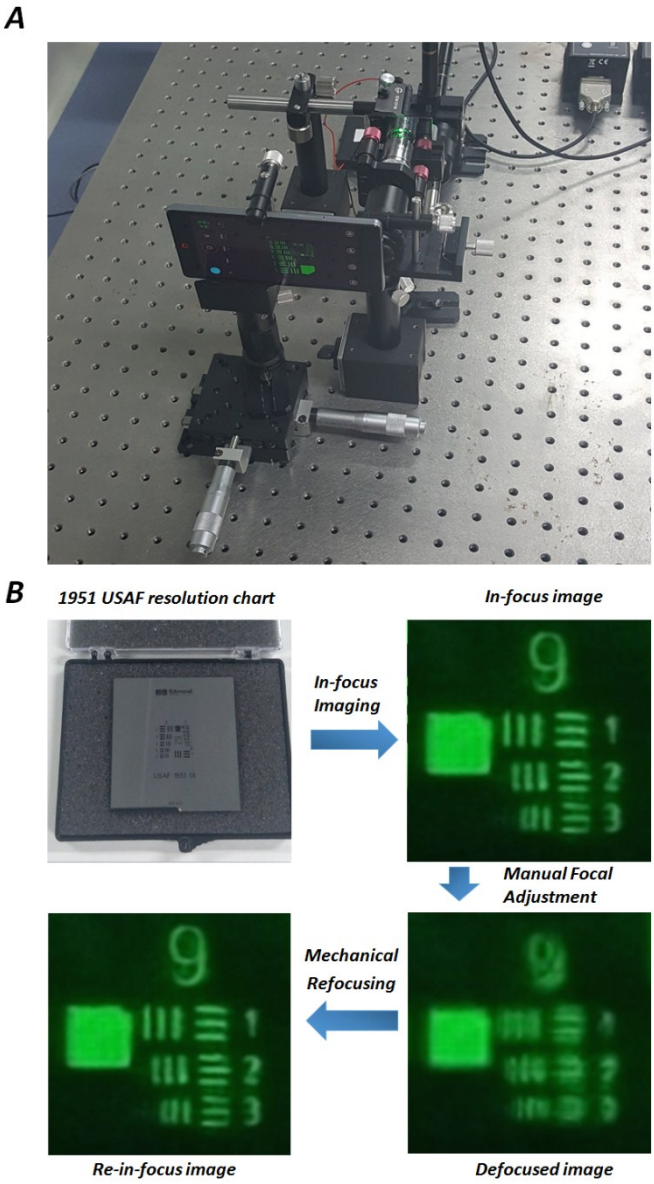

Figure S2. (A) Smartphone based hand-held quantitative phase microscope system. (B) Defocusing distance calibration process.

Additionally, Figure S3 shows quantitative calibration for both over-focus and under-focus cases. Firstly, using the “manual focusing” function of the smartphone camera software, the focal plane was shifted. Next, multiple images were recorded since the samples was shifted along the optical axis via precision translation stage with step of 0.1 μm. In the following, Tamura coefficients of all captured images were calculated thus the in-focus image could be picked out as well as its shifting distance according to largest Tamura coefficient. It is known that the shifting distance is the

defocus interval. In practical measurements, the effective defocus distance was ~5.0 μm in sample plane with difference of 9 in "Focus" value. After quantitatively calibrating the effective defocusing distance, we used the same defocusing interval for multi-focal image capturing and then, high-accurate phase distributions can be computed via solving Poisson equation.

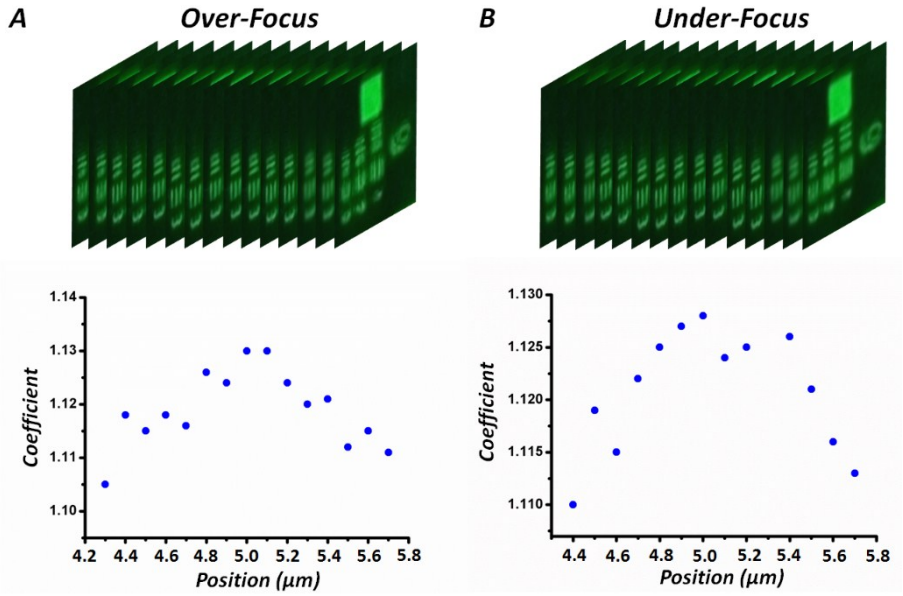

Figure S3. Quantitative calibrations for defocus distance in both (A) over-focus and (B) under-focus cases.

Phase Retrieval according to Solving Poisson Equation

In order to solve Poisson equation in Eq. (S1), FFT-based inversion solver is employed [3].

$$k\frac{\partial I(x,y)}{\partial z} = -\nabla\cdot[I(x,y)\nabla\varphi(x,y)] \qquad \text{(S1)}$$

Based on Helmoltz's theorem, we can decompose the vector field as shown in Eq. (S2), in which ψ is a continuous scalar field and ***A*** is a vector potential.

$$I\nabla\varphi = \nabla\psi + \nabla\times\mathbf{A} \qquad \text{(S2)}$$

According to Teague's theorem, the rotational term, curl ***A*** can be ignored, thus Eq. (S1) can be simplified as Eq. (S3).

$$\nabla^2\psi = -k\partial_z I \qquad \text{(S3)}$$

Supposing *f(x)* is a function, we have Eq. (S4) based on Fourier transform (F).

$$\mathrm{F}\,[\partial_x^{(n)} f(x)] = \mathrm{i}^n q_x^n \mathrm{F}\,[f(x)] \qquad \text{(S4)}$$

Thus, for two dimensional system, Eq. (S4) can be rewritten into Eq. (S5), in which where *q* is the magnitude of the variable conjugate to ***r*** in the Fourier space.

$$\nabla^2 f(\mathbf{r}) = -\mathrm{F}^{-1} q^2 \mathrm{F}\,[f(\mathbf{r})] \qquad \text{(S5)}$$

According to Eq. (S5), Eq. (S2) can be derived as Eq. (S6).

$$\psi = -\mathrm{F}^{-1} q^2 \mathrm{F}\,[k\partial_z I] \qquad \text{(S6)}$$

Based on above approximation, ignoring the rotational term in Eq. (S2), we can get Eq. (S7).

$$\nabla^2\varphi = \nabla\cdot(I^{-1}\nabla\psi) \qquad \text{(S7)}$$

Utilizing Eq. (S5) again we can get the solution of the phase.

$$\varphi = -\mathsf{F}^{-1}q^2\mathsf{F}\,[\nabla\cdot(I^{-1}\nabla\psi)] \qquad \text{(S8)}$$

Self-developed Software for Phase Retrieval in Computer Platform

Figure S4 shows the interface of the self-developed software for phase retrieval in computer platform based on MATLAB. Similar to the Android application, firstly, all over-focus, in-focus and under-focus images are read in. Next, necessary parameters should be input for following phase retrieval. Finally, quantitative phase distribution can be calculated by solving Poisson equation.

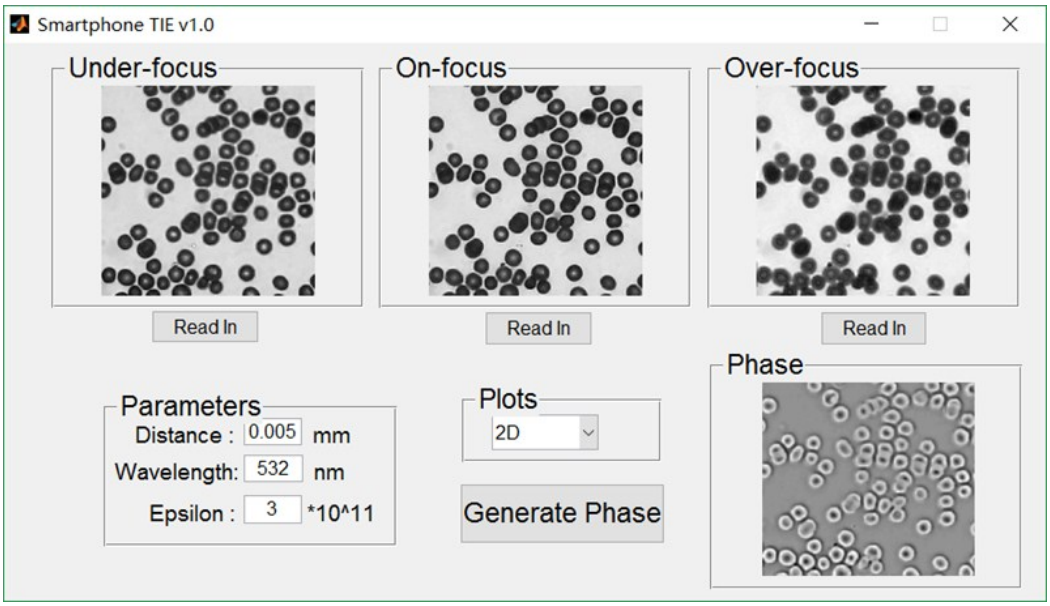

Figure S4. Interface of the self- developed software for phase retrieval in computer platform.

Surface Profile of Random Phase Plate Measured by AFM

Figure S5 shows steps of random phase plate in two different field of views measured by AFM (Agilent, US). The average height difference between two steps is ~604 nm. Considering the refractive index of the glass as 1.516 and central illumination wavelength of 620 nm, phase difference is ~π, which coincides with the results obtained by TIE.

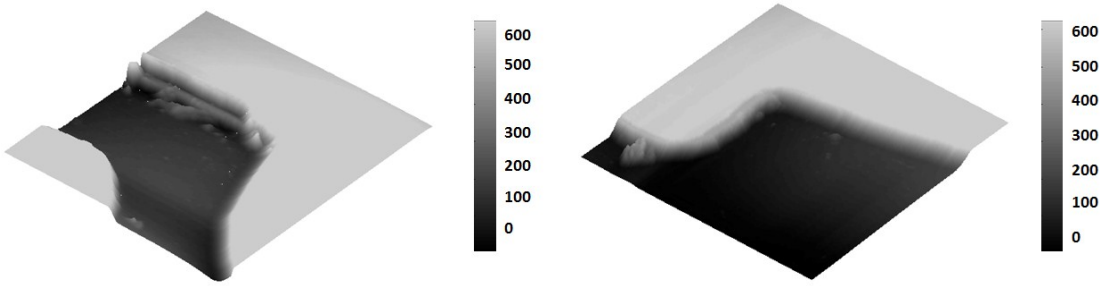

Figure S5. Surface profile of random phase plate measured by AFM.

Error Analysis in Phase Retrieval based on TIE

Error analysis in phase retrieval based on TIE is illustrated in Figure S6 using numerical simulations. Figure S6(A) to S6(C) are over-focus, in-focus and under-focus intensities, respectively. Additionally, Figure S6(D) is the setting phase. All the parameters used in numerical simulations were according to practical measurements, such as pixel size and defocus interval. The actual intervals between in-focus and defocus images were 5.1 μm, however, if in phase retrieval, the intervals were mistaken for 5.0 μm, indicating a relative error of ~2%. Figure S6(E) shows the recovered phase using the correct defocus interval, while Figure S6(F) shows the recovered phase using the incorrect defocus interval. In order to quantitatively calibrate the error induced by inaccurate defocus interval, relative error of phase was adopted to evaluate accuracy of retrieved information. It shows the relative error between Figure S6(D) and Figure S6(E) is 2.22%, while that between Figure S6(D) and Figure S6(F) is 2.30%, indicating an error increase of 3.6%. The quantitative analysis shows that the defocus error can decrease phase retrieval accuracy, however, not losing much accuracy.

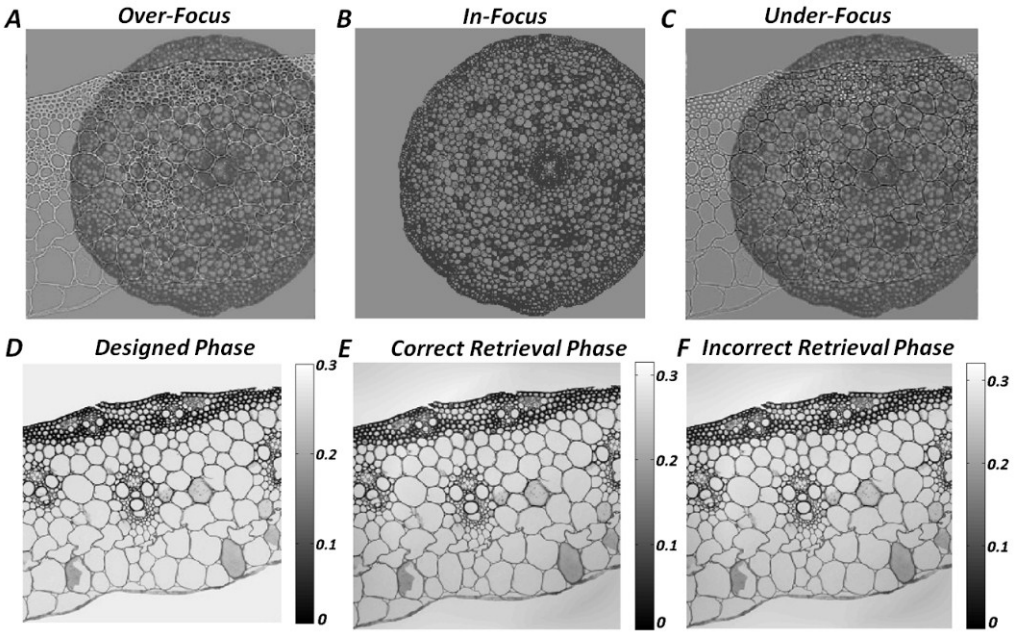

Figure S6. Error analysis in phase retrieval based on TIE. (A)-(C) Over-focus, in-focus and under-focus intensities with intervals of 5.1 μm. (D) Original setting phase. (E) Recovered phase using the correct defocus interval. (F) Recovered phase using the incorrect defocus interval of 5.0 μm.

Automatic Cellular Recognition and Statistical Analysis

According to retrieved quantitative phase distribution, automatic cellular recognition can be realized as shown in Figure S7. Noting that in order to track single cell only, adhesive cells are excluded. After cellular recognition and localization, detailed cellular parameters as areas, volumes, perimeters and roundness can be computed and statistically analyzed.

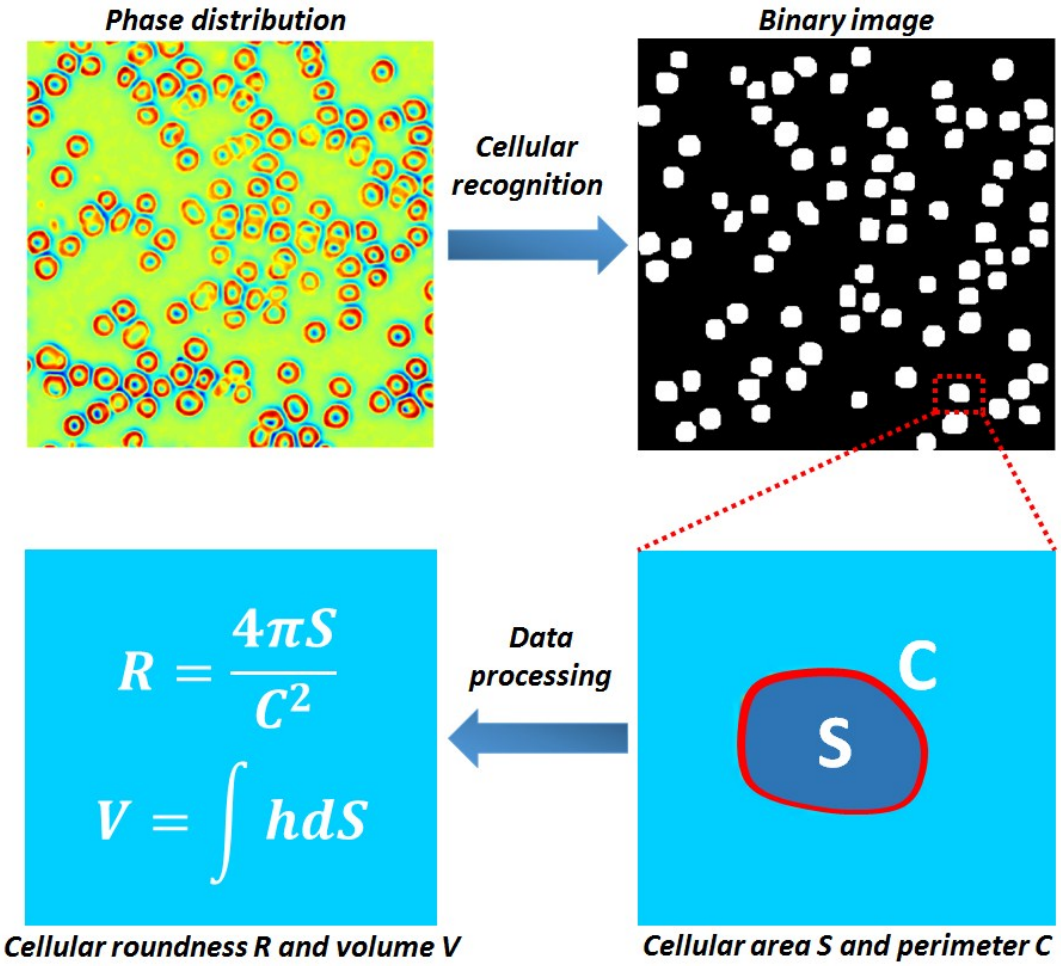

Figure S7. Flow chart of automatic cellular recognition and statistical analysis.

References

[1] P. Memmolo, C. Distante, M. Paturzo, A. Finizio, P. Ferraro, and B. Javidi, "Automatic focusing in digital holography and its application to stretched holograms," Optics Letters 36, 1945-1947 (2011).

[2] X. Tian, X. Meng, W. Yu, X. Song, L. Xue, C. Liu, and S. Wang, "In-focus quantitative intensity and phase imaging with the numerical focusing transport of intensity equation method," Journal of Optics 18, 105302 (2016).

[3] T. Gureyev and K. Nugent, "Rapid quantitative phase imaging using the transport of intensity equation," Optics Communications 133, 339-346 (1997).